PCCP

Accepted Manuscript

ROYAL SOCIETY OF CHEMISTRY

www.rsc.org/pccp

Physical Chemistry Chemical Physics
CREATED USING THE RSC LaTeX PCCP ARTICLE TEMPLATE – SEE www.rsc.org/electronicfiles FOR DETAILS
ARTICLE TYPE www. rsc.org/xxxxxx | XXXXXXXX

Strong Enhancement of Parity Violation Effects in Chiral Uranium Compounds

Michael Wormit,*[a] Małgorzata Olejniczak,[b†] Anna-Lena Deppenmeier,[c] Anastasia Borschevsky,[c,d] Trond Saue,[b] and Peter Schwerdtfeger[c]

Received Xth XXXXXXXXXX 20XX, Accepted Xth XXXXXXXXX 20XX
First published on the web Xth XXXXXXXXXX 200X
DOI: 10.1039/b000000x

The effects of parity violation (PV) on the vibrational transitions of chiral uranium compounds of the type N≡UXYZ and N≡UHXY (X, Y, Z = F, Cl, Br, I) are analysed by means of exact two-component relativistic (X2C) Hartree-Fock and density functional calculations using NUFClI and NUHFI as representative examples. The PV contributions to the vibrational transitions were found to be in the Hz range, larger than for any of the earlier proposed chiral molecules. Thus, these systems are very promising candidates for future experimental PV measurements. A detailed comparison of the N≡UHFI and the N≡WHFI homologues reveals that subtle electronic structure effects, rather than exclusively a simple Z^5 scaling law, are the cause of the strong enhancement in PV contributions of the chiral uranium molecules.

1 Introduction

The breakdown of left-right symmetry at the macroscopic and microscopic level, the latter due to parity violation (PV), is fundamental to chemistry and physics. For example, the distinct symmetry breaking in nature leading to single handedness of chiral biomolecules in living species (biomolecular homochirality), i.e. to left-handed amino-acids and right-handed sugars, is believed to be one of the necessary conditions for the existence of life.[1] While the emergence of biomolecular homochirality is not yet well understood, the role of PV effects as the cause of this distinct symmetry breaking is currently being discussed. The ground state of a chiral molecular system with a double-minimum potential connecting the two enantiomers along the inversion path can be considered as a symmetry broken entangled state mixing both positive and negative parity states, the latter states being pure states for a quantum system with a parity conserving Hamiltonian. The existence of such symmetry-broken states for chiral molecules has also been debated intensively in the past.[2] Moreover, experimental confirmation of PV effects in the spectra of chiral molecules is of fundamental importance to test the validity of the Standard Model and to gain understanding into the biomolecular homochirality phenomenon.[3–7]

High-resolution spectroscopy experiments to measure the tiny energy difference between enantiomers in chiral molecules gave so far zero results (within statistical uncertainty).[8,9] However, molecular beam spectroscopy using a two-photon Ramsey-fringes experiment is expected to reach the sub-Hertz accuracy regime where PV effects are expected to be found.[3,10] The task of quantum chemists is to guide experiments in the search for suitable chiral candidates for such measurements. Nuclear spin-independent PV energy contributions are predicted to scale as Z^5 (Z being the nuclear charge),[11–15] therefore, the search for chiral molecules focuses on heavy element containing compounds. It is, however, by no way trivial to find suitable molecules containing heavy elements that are chiral, thermodynamically stable, and accessible to high-resolution experiments in a certain frequency range.[3,4,16] A number of chiral molecules have been suggested, most recently chiral tungsten compounds containing a W≡N triple bond[17,18] and chiral oxorhenium species,[4,19,20] both with stretching frequencies conveniently lying in the operating range of the CO_2 laser (900 - 1100 cm^{-1}) used for these high precision spectroscopic measurements.

Recently, Andrews and co-workers reported uranium-atom reactions with NF_3 and PF_3 to prepare terminal uranium nitride and phosphide functional groups.[21] The (achiral) N≡UF_3 product has a N≡U stretching frequency of 938 cm^{-1}, which is in the lower frequency range of the CO_2 laser. Chiral compounds of the form N≡UXYZ and N≡UHXY (X, Y, Z = F, Cl, Br, I) could thus be suitable can-

[a] *Interdisciplinary Center for Scientific Computing, Heidelberg University, Im Neuenheimer Feld 368, D-69120 Heidelberg, Germany. Fax: +49-(0)6221-54-8868; Tel: +49-(0)6221-54-8781; E-mail: michael.wormit@iwr.uni-heidelberg.de*
[b] *Laboratoire de Chimie et Physique Quantiques, Université de Toulouse 3 (Paul Sabatier), 118 route de Narbonne, 31062 Toulouse, France.*
[c] *Centre of Theoretical Chemistry and Physics, Massey University, Auckland, New Zealand.*
[d] *Helmholtz Institute Mainz, Mainz D-55128, Germany.*
[†] *Present address: Laboratoire PhLAM CNRS UMR 8523, Université de Lille 1, Bât P5, F-59655 Villeneuve d'Ascq Cedex, France.*

didates for future PV measurements. We have therefore investigated PV effects in these molecules using Hartree-Fock and density functional theory based on the exact two-component relativistic (X2C) Hamiltonian.[22] In addition to estimating the magnitude for the PV shift in the vibration frequency in these systems, we have also attempted to gain a better understanding of the electronic nature of these PV effects. To this end, we have performed an in-depth analysis of the orbital contributions to the PV shifts in the N≡UHFI molecule in comparison with its lighter homologue, N≡WHFI.

2 Theory

The PV energy contribution E_{PV} at a given molecular geometry is obtained as an expectation value, which at the relativistic 4-component SCF level reads

$$E_{PV} = \sum_{\mathrm{K}} E_{PV}^{\mathrm{K}}; \quad E_{PV}^{\mathrm{K}} = \sum_{i}^{N_{occ}} \langle \psi_i | H_{PV}^{\mathrm{K}} | \psi_i \rangle , \tag{1}$$

where ψ_i are the occupied Hartree-Fock (HF) or Kohn-Sham (KS) orbital spinors, and the index K labels the individual atoms. The total PV energy is a sum over atomic contributions E_{PV}^{K} with the corresponding nuclear spin-independent P-odd Hamiltonian expressed as

$$H_{PV}^{\mathrm{K}} = \frac{G_F}{2\sqrt{2}} Q_W^{\mathrm{K}} \gamma^5 \rho^{\mathrm{K}}(\mathbf{r}). \tag{2}$$

Here, $G_F = 2.22249 \times 10^{-14}\, E_h a_0^3$ is the Fermi coupling constant, ρ^{K} is the normalized nuclear charge density of atom K, in the present work represented by a Gaussian distribution,[23] and γ^5 is the pseudochirality Dirac matrix connecting the large and the small Dirac components,

$$\gamma^5 = \begin{pmatrix} 0_2 & 1_2 \\ 1_2 & 0_2 \end{pmatrix}, \tag{3}$$

with 1_2 and 0_2 being the 2×2 identity and zero matrix, respectively. The weak charge of nucleus K is given by $Q_W^{\mathrm{K}} = -N^{\mathrm{K}} + Z^{\mathrm{K}}(1 - 4\sin^2\theta_W)$, where N^{K} and Z^{K} are the number of neutrons and protons of nucleus K, respectively. The Weinberg mixing angle, θ_W, is given by $\sin^2\theta_W = 0.2319$.[24]

The PV vibrational shift, corresponding to the tiny displacement of vibrational lines between two enantiomers of a chiral molecule due to parity violation, is given by

$$\Delta\nu_{m\to n}^{PV} = \frac{2}{h}(P_m - P_n), \tag{4}$$

where $P_n = \langle n | E_{PV}(Q) | n \rangle$ is the value of E_{PV} in the vibrational state n of the selected mode with normal coordinate Q. The above expression is approximate in that it neglects the coupling between the vibrational modes.

The vibrational expectation values P_n can be obtained by directly solving the vibrational problem for the selected normal mode, for instance by the numerical Numerov-Cooley procedure.[25–27] However, for the purpose of an analysis a perturbative approach provides a more detailed insight. The vibrational expectation value can be approximated as

$$\begin{aligned} P_n \approx P^{[0]} &+ \frac{1}{2}P^{[2]}\left(\frac{\hbar}{\mu\omega_e}\right)\left(n+\frac{1}{2}\right) \\ &- \frac{1}{2}P^{[1]}V^{[3]}\left(\frac{\hbar}{\mu\omega_e}\right)^2 \frac{\left(n+\frac{1}{2}\right)}{\hbar\omega_e} \\ &- \frac{1}{16}P^{[2]}V^{[4]}\left(\frac{\hbar}{\mu\omega_e}\right)^3 \frac{n^2+n+\frac{1}{2}}{\hbar\omega_e}, \end{aligned} \tag{5}$$

where $V^{[n]}$ and $P^{[n]}$ are the MacLaurin expansion coefficients of the potential energy curve and of the property (E_{PV}) curve along the normal coordinate Q, truncated to fourth and second order, respectively. μ refers to the reduced mass of the selected normal mode, while ω_e is the angular harmonic frequency of the mode. Setting the quartic force constant $V^{[4]}$ to zero we obtain[28,29]

$$\Delta\nu_{0\to n}^{PV} = \frac{n}{h}\left(\frac{\hbar}{\mu\omega_e}\right)\left(P^{[2]} - P^{[1]}V^{[3]}\frac{1}{\mu\omega_e^2}\right), \tag{6}$$

which is the perturbative expression for the PV vibrational shift that will be employed in the present work. This expression shows that when higher-order contributions are ignored, the PV vibrational shift $\Delta\nu_{0\to n}^{PV}$ is proportional to the vibrational quantum number n, in line with previous observations.[18,30,31] Moreover, experience shows that $\Delta\nu_{0\to 1}^{PV;\mathrm{K}} \ll E_{PV}^{\mathrm{K}}/h$ for fundamental vibrational transitions.[30,32]

To obtain a deeper insight into the nature of the PV vibrational shift we also carry out projection analysis, as introduced in a previous study.[15] The molecular orbitals of Eq. (1) are decomposed into precomputed atomic orbitals,

$$|\psi_i\rangle = \sum_{\mathrm{A}} \sum_{p\in\mathrm{A}} \left|\psi_p^{\mathrm{A}}\right\rangle c_{pi}^{\mathrm{A}} + \left|\psi_i^{\mathrm{pol}}\right\rangle. \tag{7}$$

Typically only the occupied atomic orbitals will be employed; the part of the molecular orbital which is not spanned by the selected set of atomic orbitals is denoted the polarization contribution ψ_i^{pol}, which by construction is orthogonal to the selected atomic orbitals.

The PV energy associated with center M can then be expressed as

$$E_{PV}^{M} = \sum_{\mathrm{A}}\sum_{p\in\mathrm{A}}\sum_{\mathrm{B}}\sum_{q\in\mathrm{B}} \left\langle \psi_p^{\mathrm{A}} \right| H_{PV}^{M} \left| \psi_q^{\mathrm{B}} \right\rangle D_{qp}^{\mathrm{BA}} + (\mathrm{pol})$$

$$\text{with} \quad D_{qp}^{\mathrm{BA}} = \sum_{i}^{N_{occ}} c_{qi}^{\mathrm{B}} c_{pi}^{\mathrm{A}*}, \tag{8}$$

allowing a distinction between intraatomic (A = B) and interatomic (A $\neq$ B) contributions and even identifying individual contributions from orbital pairs.

3 Computational Methods

The geometries of the N≡UXYZ and N≡UHXY molecules (X, Y, Z=F, Cl, Br, I) were optimized at the B3LYP hybrid functional level of theory[33,34] using the GAUSSIAN09 program package.[35] For the lighter elements (H, N, F, and Cl) uncontracted augmented correlation-consistent valence triple-ζ (AVTZ) Gaussian basis sets were used.[36,37] For Br, I, and U we employed the AVTZ basis sets in conjunction with the Stuttgart small-core energy consistent scalar relativistic pseudopotentials (SRPPs)[38,39] in order to account for scalar-relativistic effects. The normal modes and the harmonic frequencies of the U≡N stretching mode were obtained by the same computational protocol. The anharmonic frequency analysis was performed using perturbation theory as described in Refs. 40,41 and as implemented in Gaussian09.[35]

The calculations of E_{PV} at optimized geometries were carried out using the DIRAC10 computational package.[42] In order to reduce the computational effort, the four-component Dirac-Coulomb Hamiltonian was replaced by the exact two-component relativistic Hamiltonian (X2C).[22] Using this scheme, the contribution of the two-electron spin-same-orbit coupling is introduced in a mean field fashion using the AMFI code[43] as implemented in the DIRAC10 program package. It was shown[18] that the X2C PV energies reproduce the four-component results within $\simeq 3\%$ for the NWHXY and NWXYZ compounds, which validates our use of this approximation here. For comparison, the calculations were performed both at the Hartree-Fock (HF) and the density functional theory (DFT) level. For the latter calculations we employed the LDA, PBE, and B3LYP functionals, as well as the Coulomb-attenuated B3LYP functional,[44] the parameters of which were adjusted by Thierfelder *et al.*[45] to reproduce the PV energy shifts obtained at the coupled cluster level. The parameters of the adjusted functional, denoted CAM-B3LYP*, are $\alpha = 0.20$, $\beta = 0.12$, and $\mu = 0.90$. Dunning's AVTZ basis sets were employed in their uncontracted form for the lighter elements (H, N, F, and Cl). For the heavier atoms we used the Faegri's dual family basis sets,[46] augmented with higher orbital momentum and diffuse functions to obtain the sets $21s17p15d4f2g$, $22s19p15d4f3g$, and $26s23p17d4f3g$ for bromine, iodine, and uranium, respectively. In all calculations the most abundant isotopes of those elements ^{7}9Br, ^{1}27I, and ^{2}38U were adopted.

We selected two systems, NUHFI and NUFClI, for which we calculated the PV vibrational shifts. The PV energy $E_{PV}(Q)$ was calculated pointwise along the normal coordinate Q of the U≡N stretching mode and fitted to a polynomial. The potential energy curves were obtained, using the B3LYP functional, in the same range, corresponding to a displacement of ± 0.5 Å along the normal coordinate. Vibrational expectation values P_n were then calculated using single mode vibrational wave functions obtained by the Numerov-Cooley procedure,[25–27] and using Eq. (6).

The comparative study of the PV vibrational shifts of the homologous uranium and tungsten chiral molecules NUHFI and NWHFI[18] was performed using projection analysis.[15] These calculations were carried out at the 4-component relativistic DFT level using the B3LYP functional and the uncontracted VTZ-type basis sets (Dunning's cc-pVTZ[47] basis sets for H, F and N atoms and Dyall's VTZ basis for I,[48] W[49] and U[50] atoms).

4 Results and discussion

The harmonic ($\tilde{\omega}_e$) and the fundamental ($\tilde{\nu}$) vibrational wavenumbers of the stretching of the triple N≡U bond, together with the bond length, R_{NU}, for the molecules under study are shown in Table 1. To assess the accuracy of our predictions of the molecular properties of these compounds, we also calculated the vibrational wavenumbers of the NUF_3 molecule, which has been experimentally investigated by Andrews *et al.*[21] The fundamental wavenumber of the N≡U stretching mode, measured using matrix infrared spectroscopy, is 938 cm^{-1}, compared to our calculated value $\tilde{\nu} = 994$ cm^{-1} for the free molecule. Thus, our result is in reasonably good agreement with the experiment, exceeding the measured value by about 5%. The N≡U stretching wavenumbers of the compounds studied here are very close in values and are all in the operating range of the CO_2 laser.[8,51] Furthermore, our calculations suggest that no other modes possess wavenumbers close to those of the N≡U stretching mode. The closest normal modes are the U−F stretching and bending modes at about 600 cm^{-1} and the U−H stretching mode at about 1500 cm^{-1} for the fluorine- and hydrogen-containing systems (Figure 1).

Table 2 contains the parity violation energies, E_{PV}, at equilibrium geometries, obtained at the HF and DFT (LDA, PBE, B3LYP, and CAM-B3LYP*) level. Here we choose the *R*-enantiomer for the hydrogen-containing systems, and the *S*-enantiomer for the remaining molecules. The substitution of the hydrogen by a halogen leads to a change in the priority of the ligands, according to the Cahn-Ingold-Prelog rules.[52] For consistency in our E_{PV} results we therefore chose the chiral configuration where all HF values are negative in sign. Table 2 shows that for the hydrogen-containing compounds the PV energies obtained with HF are generally the lowest while those obtained with LDA are the highest, and the spread of these values is quite large. The exact value can be expected to be in between these two limiting cases.[30,53] For the compounds not

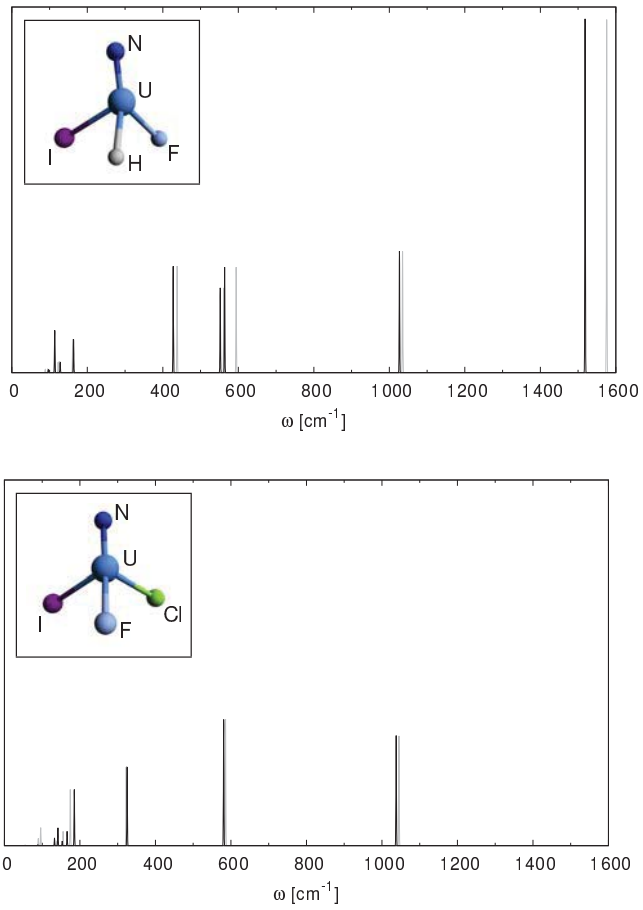

Fig. 1 Vibrational spectrum of NUHFI (top) and NUFClI (bottom). The vibrational frequencies are displayed in harmonic approximation (light), as well as including anharmonic contributions (dark).

containing hydrogen this variation is far less pronounced. Surprisingly, here B3LYP yields the highest PV energies while the lowest PV energies are obtained with both HF and LDA. We also mention that the PV contributions E_{PV}^{U} associated with the heaviest atom uranium dominate the total PV energy for all systems and all methods applied, and in most cases this contribution is more than 95% of the total PV energy (only for NUHClI and NUHBrI, when calculated using the LDA or PBE functionals, the contribution can be as low as 68% of the total PV energy).

Table 3 reports the PV vibrational shifts $\Delta\nu_{PV}^{0\to1}$ (Eq. (4)) associated with the N≡U stretching mode of the NUHFI and NUFClI molecules, with respect to the *R*- and *S*-enantiomers, respectively, obtained by the Numerov-Cooley procedure. For the $0 \to 1$ fundamental transition we find shifts in the range from 13.0 to 38.6 Hz for NUHFI and from -6.9 to 2.7 Hz

Table 1 Calculated bond lengths R_{NU} and harmonic ($\tilde{\omega}_e$) and fundamental ($\tilde{\nu}$) vibrational wavenumbers of the N≡U bond resulting from anharmonic frequency analysis.

	R_{NU} [Å]	$\tilde{\omega}_e$ [cm^{-1}]	$\tilde{\nu}$ [cm^{-1}]
NUHFCl	1.699	1028.1	1016.9
NUHFBr	1.698	1031.4	1021.8
NUHFI	1.697	1035.0	1026.8
NUHClBr	1.698	1040.3	1032.9
NUHClI	1.697	1043.3	1034.5
NUHBrI	1.696	1046.2	1039.1
NUClBrI	1.695	1035.6	1029.0
NUFClBr	1.691	1042.2	1033.4
NUFClI	1.690	1045.1	1037.7
NUFBrI	1.689	1047.6	1039.8

Table 2 Parity violating energies E_{PV} (Hz) at equilibrium geometry obtained using LDA, PBE, B3LYP, and CAM-B3LYP* functionals as well as HF in combination with the X2C Hamiltonian.

Molecule	LDA	PBE	B3LYP	CAM-B3LYP*	HF
R−NUHFCl	245.9	209.2	59.0	−45.8	−120.4
R−NUHFBr	250.6	210.6	−19.7	−157.3	−207.5
R−NUHFI	188.5	168.2	−230.1	−424.4	−403.1
R−NUHClBr	18.9	19.5	−62.4	−97.9	−112.3
R−NUHClI	−7.6	7.0	−248.0	−339.9	−356.8
R−NUHBrI	−24.5	−11.7	−184.2	−240.8	−246.3
S−NUClBrI	−33.3	−25.8	−21.6	−21.8	−26.4
S−NUFClBr	−25.0	−20.9	−13.0	−19.7	−35.6
S−NUFClI	−91.3	−77.0	−45.2	−58.0	−106.2
S−NUFBrI	−68.1	−56.8	−34.3	−42.2	−71.6

for NUFClI, more than an order of magnitude higher than for earlier candidates of similar structure, the NWXYZ set of molecules.[18]

In order to understand the underlying mechanism for the very large PV vibrational shifts observed for the uranium compounds we have undertaken a detailed comparison of PV contributions in the NUHFI molecule and in its tungsten homologue NWHFI. The PV shifts $\Delta\nu_{PV}^{0\to1}$ with respect to the *R*-enantiomers, calculated at the 4-component relativistic DFT level (B3LYP) are reported in Table 4. The shifts have been calculated using the perturbative formula of Eq. (6) and the parameters appearing in this formula ($V^{[3]}$, $P^{[1]}$, and $P^{[2]}$) are also reported in Table 4. The values for the two systems are indeed very different, with the PV shift of the uranium compound being more than forty times larger than that of its tungsten homologue. It should be noted that the reduced mass, μ, the harmonic wavenumber, $\tilde{\omega}_e$, and the cubic force constant, $V^{[3]}$, are quite similar for the M≡N stretch mode of the two molecules, meaning that the large difference in the PV vibrational shifts stems almost entirely from the first and the

Table 3 Vibrational transition wavenumbers $\Delta\tilde{\nu}_e$ [cm^{-1}] of the N≡U stretching mode of *R*-NUHFI and *S*-NUFClI and the PV vibrational shifts $\Delta\nu_{PV}^{0\to n}$ [mHz] of these modes. The wavenumbers have been calculated from the B3LYP potential energy surface along the stretching mode using the Numerov-Cooley procedure.

Method	$0\to1$	$0\to2$	$0\to3$	$0\to4$
R−NUHFI				
$\Delta\tilde{\nu}_e$ B3LYP	1028.8	2050.2	3064.2	4070.7
$\Delta\nu_{PV}$ LDA	38591.5	80146.1	124745.5	172392.4
$\Delta\nu_{PV}$ PBE	36328.6	74983.3	115949.5	159147.4
$\Delta\nu_{PV}$ B3LYP	22101.8	46280.1	72608.9	101141.9
$\Delta\nu_{PV}$ CAM-B3LYP*	12962.7	27430.8	43445.9	61031.1
S−NUFClI				
$\Delta\tilde{\nu}_e$ B3LYP	1037.8	2068.3	3091.4	4107.1
$\Delta\nu_{PV}$ LDA	-6905.5	-14101.1	-21562.8	-29257.0
$\Delta\nu_{PV}$ PBE	-6585.1	-13343.3	-20256.8	-27303.5
$\Delta\nu_{PV}$ B3LYP	-375.3	-600.1	-646.1	-482.9
$\Delta\nu_{PV}$ CAM-B3LYP*	2748.6	5714.1	8932.4	12444.6

second property derivatives $P^{[1]}$ and $P^{[2]}$. The cubic force constant $V^{[3]}$ is negative for both molecules, as one could expect, for instance, by considering a Morse potential. Looking at Eq. (6) it is seen that for negative $V^{[3]}$ the anharmonic contribution, proportional to $P^{[1]}$, will reinforce the harmonic contribution, proportional to $P^{[2]}$. Indeed, for both molecules the anharmonic contribution constitutes about half of the total PV vibrational shift.

Table 4 PV vibrational shifts $\Delta\nu_{PV}^{0\to1}$ of the N≡U stretching mode of *R*-NMHFI (M = W, U) molecules, calculated at the 4-component relativistic DFT level (B3LYP). In addition, the harmonic contribution $\Delta\nu_{PV}^{harm}$, reduced mass μ, harmonic wavenumber $\tilde{\omega}_e$, cubic force constant $V^{[3]}$, property derivatives $P^{[n]}$, and individual contributions $\Delta\nu_{PV}^{X}$ of each atom (X = F, H, I, N, U, W) are shown.

NMHFI		M = W	M = U
$\Delta\nu_{PV}^{0\to1}$	(mHz)	529.9	22070.6
$\Delta\nu_{PV}^{harm}$	(mHz)	245.8	12016.5
μ	(Da)	14.94	14.53
$\tilde{\omega}_e$	(cm^{-1})	1145.8	1065.42
$V^{[3]}$	($E_h a_0^{-3}$)	-2.02	-1.81
$P^{[1]}$	($E_h a_0^{-1}$)	$2.28\cdot10^{-15}$	$6.93\cdot10^{-14}$
$P^{[2]}$	($E_h a_0^{-2}$)	$5.31\cdot10^{-15}$	$2.35\cdot10^{-13}$
$\Delta\nu_{PV}^{F}$	(mHz)	-0.1	0.4
$\Delta\nu_{PV}^{H}$	(mHz)	0.0	0.0
$\Delta\nu_{PV}^{I}$	(mHz)	162.4	-100.9
$\Delta\nu_{PV}^{N}$	(mHz)	0.0	0.3
$\Delta\nu_{PV}^{M}$	(mHz)	367.7	22170.7

In Table 4 we also list the contribution $\Delta\nu_{PV}^{X}$ of each atom (X = F, H, I, N, U, W) to the total vibrational shift. Interestingly, although the contribution from iodine is of the same order of magnitude in the two molecules, it opposes the total shift in NUHFI and amplifies it in the tungsten homologue. Clearly the large difference in vibrational shift between NUHFI and NWHFI arises from the contribution from the central metal atom M, which we will focus on in the following.

Table 5 Decomposition of $\Delta\nu_{PV}^{M}$ (M = W, U) by projection analysis. All quantities are in mHz.

	M = W	M = U
Intra-atomic	89.0	21826.6
Inter-atomic	-2.0	35.9
Polarization	280.7	308.2
Total	367.7	22170.7

In Table 5 we have decomposed the contribution $\Delta\nu_{PV}^{M}$ into intra- and interatomic as well as polarization contributions (Eq. (8)) using our projection analysis. The inter-atomic contribution is negligible for both molecules, as can be expected from the atomic nature of the operator, Eq. (2). For NUHFI $\Delta\nu_{PV}^{U}$ is completely dominated by the intraatomic contribution. Unfortunately, for NWHFI $\Delta\nu_{PV}^{W}$ is dominated by the polarization contribution, which complicates the analysis by blurring the distinction between the intra- and the inter-atomic contributions. In fact, the original projection analysis for both species used the occupied atomic orbitals of the ground state configurations of the neutral atoms. For NWHFI $\Delta\nu_{PV}^{W}$ then decomposes into a polarization contribution of 1372.4 mHz and an intra-atomic contribution of the opposite sign (-1002.7 mHz), rendering the analysis essentially meaningless. To alleviate this problem we explored various strategies for polarizing the atomic orbitals within the molecule, including the Intrinsic Atomic Orbitals (IAO) of Knizia,[54] but no approach was successful. The IAOs approach, for instance, eliminates completely the polarization contribution, but at the price of introducing artificially large inter-atomic contributions to the PV shifts. The results for NWHFI shown in Table 5 and in the following have been obtained by careful tuning of the generation and selection of tungsten atomic orbitals for analysis, more precisely by generating the AOs from the configuration $[\mathrm{Xe}]4f^{14}5d^{4.0}6s^{0.5}6p^{0.5}$ and including all occupied orbitals in the analysis. This result is not perfect, but sufficient for more detailed analysis.

The general expression for the PV energy associated with the metal center M, in the framework of projection analysis, is given by Eq. (8), but Table 5 shows that if polarization contributions are excluded, the energy is very well approximated by

$$E_{PV}^{M} \approx \sum_{p,q\in M} \langle \psi_p^M | H_{PV}^M | \psi_q^M \rangle D_{qp}^{MM} \qquad (9)$$

In a previous analysis[15] it was shown that for a single center M atomic orbitals $\psi^{\mathrm{M}}_{\kappa,m_j}$ couple through the PV operator H^{M}_{PV} in a chiral molecular field, only if they have the same m_j value as well as the same absolute value of κ, but of opposite sign. When in addition the normalized charge density ρ^{M} is represented by a Dirac delta function, only the $s_{1/2}$ and the $p_{1/2}$ orbitals form non-zero matrix elements,[55,56] which are also the dominant contributions when an extended nuclear model is chosen. Previous studies[11–13] suggest that the PV energy E^{M}_{PV} scale as Z^5_{M}. It has also been estimated[57–59] that atomic matrix elements $\langle \psi^{\mathrm{M}}_p | H^{\mathrm{M}}_{PV} | \psi^{\mathrm{M}}_q \rangle$ scale as Z^3_{M}. This suggests that the density matrix D^{MM} of Eq. (9), describing the mixing of atomic $s_{1/2}$ and the $p_{1/2}$ orbitals in the molecule, scales as Z^2_{M}, which was indeed explicitly shown for the H_2X_2 series of molecules (X = O, S, Se, Te, Po).[15] However, there is no simple way of deducing the magnitude of PV vibrational shifts from Eq. (9). In fact, Eq. (6) clearly shows that the PV energy at the equilibrium geometry does not contribute to the PV shift at all. Thus, in order to understand the large difference between PV shifts of NWHFI and NUHFI we shall analyze the perturbation expression Eq. (6) for which no simple scaling rules are known. Based on the projection analysis we may express the PV shift associated with the metal center M of NMHFI as

$$h\Delta\nu^{\mathrm{M}}_{PV} \approx \left(\frac{\hbar}{\mu\omega_e}\right) \sum_{p,q\in \mathrm{M}} \left(D^{[2]}_{pq} - D^{[1]}_{pq} V^{[3]} \frac{1}{\mu\omega_e^2}\right) \langle \psi^{\mathrm{M}}_p | H^{\mathrm{M}}_{PV} | \psi^{\mathrm{M}}_q \rangle \quad (10)$$

where $D^{[n]}_{pq}$ are the elements of the nth derivative of the density matrix in the basis of pre-calculated atomic orbitals (see Eq. (8)) with respect to the normal coordinate Q of the M≡N stretching mode.

It is important to realize that the atomic matrix elements $\langle \psi^{\mathrm{M}}_p | H^{\mathrm{M}}_{PV} | \psi^{\mathrm{M}}_q \rangle$ are strictly geometry independent and can in principle be precalculated; all the effects of molecular vibrations and electronic structure are encoded in $D^{[n]}$. In Tables 6 and 7 we give the reduced PV property elements

$$M^{PV}_{n,n'} = \langle ns_{1/2} | \gamma_5 \rho^{\mathrm{M}} | n' p_{1/2} \rangle \quad (11)$$

for tungsten and uranium, respectively. With a proper choice of phase they are all real and positive.[15] In their seminal work Bouchiat and Bouchiat[55] concluded using quantum defect theory[60] that the non-relativistic reduced PV property elements scale as Z^2, which when multiplied with the weak charge Q^A gives the predicted Z^3 scaling of the atomic matrix elements. In addition they introduced a relativistic scaling factor which can be expanded in orders of the nuclear charge, the zeroth-order term being, as expected, close to unity (0.96). In the present case, the Z^2 scaling law suggests that the reduced matrix elements of uranium should be a factor $(92/74)^2$=1.55 larger than those of tungsten. The relativistic scaling factor is 6.04 and 15.42 for tungsten and uranium, respectively, which suggests that the atomic matrix elements $M^{PV}_{n,n'}$ of uranium should overall be almost a factor four (3.93) larger than those of tungsten. A comparison of Tables 6 and 7 shows that this scaling law does not hold; for instance we find that $M^{PV;\mathrm{U}}_{6,5}/M^{PV;\mathrm{W}}_{6,5} \sim 16$. On the other hand such a comparison is somewhat misleading since one should rather compare chemically equivalent orbital pairs, thus we find $M^{PV;\mathrm{U}}_{7,6}/M^{PV;\mathrm{W}}_{6,5} \sim 2.2$ which is more in line with the suggested scaling law, although far from perfect. An interesting observaton is that a power fit

$$M^{PV}_{n,n'} = x\left(\varepsilon_{ns_{1/2}}\varepsilon_{n'p_{1/2}}\right)^y$$

($\varepsilon_{ns_{1/2}}$ and $\varepsilon_{np_{1/2}}$ are the energies of the $ns_{1/2}$ and the $n'p_{1/2}$ orbitals) yields the fit parameters $(x,y) = (54.4, 0.49)$ and $(473.3, 0.44)$ for tungsten and uranium, respectively, suggesting that the reduced matrix elements scale linearly with the geometric mean of the orbital eigenvalues. In fact, if we carry out a *relative* least squares fit of

$$M^{PV}_{n,n'} = x\left(\varepsilon_{ns_{1/2}}\varepsilon_{n'p_{1/2}}\right)^{1/2},$$

that is, minimizing relative rather than absolute deviations, a striking linear relationship is obtained, as illustrated in Figure 2. This is different from the scaling $y = 3/4$ suggested by Bouchiat and Bouchiat[55] and therefore merits further investigation. The relative least squares fits give slopes (x) of 51.6 and 289.6 a.u. for W and U, respectively. The ratio of slopes is accordingly 5.61, which suggests that the estimate of Bouchiat and Bouchiat is reasonable when atomic matrix elements with identical geometric mean of orbital energies, rather than same principal quantum numbers, are compared.

Table 6 Reduced matrix elements $M^{PV}_{n,n'}$ of tungsten. Orbital energies ε are given in italics. All quantities are in atomic units.

W	$2p_{1/2}$ *-422.678*	$3p_{1/2}$ *-93.850*	$4p_{1/2}$ *-18.034*	$5p_{1/2}$ *-2.247*	$6p_{1/2}$ *-0.270*
$1s_{1/2}$ *-2555.075*	51543.3	25832.9	12679.5	4883.9	1343.1
$2s_{1/2}$ *-442.056*	19496.0	9771.2	4795.9	1847.3	508.0
$3s_{1/2}$ *-102.500*	9244.0	4633.0	2274.0	875.9	240.9
$4s_{1/2}$ *-21.633*	4588.2	2299.6	1128.7	434.8	119.6
$5s_{1/2}$ *-3.336*	1919.2	961.9	472.1	181.8	50.0
$6s_{1/2}$ *-0.452*	631.3	316.4	155.3	59.8	16.4

This amplification is however not sufficient to explain the order-of-magnitude difference of the PV vibrational shifts in

Table 7 Reduced matrix elements $M^{PV}_{n,n'}$ of uranium. Orbital energies ε are given in italics. All quantities are in atomic units.

U	$2p_{1/2}$ *-769.116*	$3p_{1/2}$ *-188.969*	$4p_{1/2}$ *-45.935*	$5p_{1/2}$ *-9.337*	$6p_{1/2}$ *-1.167*
$1s_{1/2}$ *-4259.622*	305622.5	158271.2	82444.2	40312.7	16720.6
$2s_{1/2}$ *-797.009*	126154.0	65330.8	34031.1	16640.2	6901.9
$3s_{1/2}$ *-201.824*	61537.9	31868.3	16600.3	8117.1	3366.7
$4s_{1/2}$ *-51.767*	32085.1	16615.8	8655.2	4232.1	1755.4
$5s_{1/2}$ *-11.625*	16153.5	8365.3	4357.5	2130.7	883.8
$6s_{1/2}$ *-1.847*	7244.7	3751.8	1954.3	955.6	396.4
$7s_{1/2}$ *-0.171*	2351.8	1217.9	634.4	310.2	128.7

Table 8 Individual orbital contributions (in mHz) to the PV vibrational shift of NWHFI

W	$2p_{1/2}$	$3p_{1/2}$	$4p_{1/2}$	$5p_{1/2}$	$6p_{1/2}$
$1s_{1/2}$	-0.1	0.4	-1.3	14.4	14.8
$2s_{1/2}$	0.2	-1.1	3.2	-34.5	-35.6
$3s_{1/2}$	-0.4	1.8	-5.3	57.9	61.5
$4s_{1/2}$	0.6	-2.7	7.7	-89.5	-109.2
$5s_{1/2}$	-0.9	3.7	-10.2	134.9	242.4
$6s_{1/2}$	7.7	-41.0	174.4	-657.8	352.8

NWHFI and NUHFI. This becomes even more clear, if we turn to Tables 8 and 9, which show the contributions of the individual orbital pairs of tungsten and uranium, respectively, to the vibrational PV shift. One immediately notices that although the core orbitals yield the largest property matrix elements, the resulting contributions to the PV shift are quite small, since there is very little mixing of the $s_{1/2}$ and the $p_{1/2}$ core orbitals, due to the fact that the spherical atomic symmetry is largely maintained in the core region. It should also be noted that the PV shift critically depends on how this mixing *changes* with molecular geometry. The single largest contribution to the NUHFI PV shift comes from the uranium subvalence $(6s_{1/2}, 6p_{1/2})$ orbital pair, followed by the $(7s_{1/2}, 6p_{1/2})$ pair. The atomic reduced PV matrix element of the latter orbital pair is multiplied by a factor of 107.0 to give a contribution of 13778.3 mHz to the PV vibrational shift. In contrast, the reduced PV matrix element of the equivalent tungsten orbital pair $(6s_{1/2}, 5p_{1/2})$ is multiplied by a factor -11.0 to give -657.8 mHz, which is the largest contribution to the NWHFI PV shift.

These observations suggest that the large difference in the PV shifts of NWHFI and NUHFI has to be attributed to subtle electronic structure effects which are not easily captured by simple scaling laws as perfectly illustrated by the above shifts. The uranium $D^{[0]}_{7s,6p}$ and tungsten $D^{[0]}_{6s,5p}$ density matrix elements are $2.1 \cdot 10^{-4}$ and $-1.2 \cdot 10^{-4}$, respectively. Their ratio corresponds to a scaling $Z^{2.6}$ which is reasonable and identical to what was found previously for the H_2X_2 series of molecules.[15] However, as already stressed, the value of the density matrix at the equilibrium molecular structure does not contribute to the PV shift, only its derivatives do (cf. Eq. (10)). The anharmonic contribution to the PV shift, proportional to $D^{[1]}$ is 3403.8 mHz and -970.7 mHz for $U_{7s,6p}$ and $W_{6s,5p}$, respectively. The ratio of these anharmonic contributions corresponds to a $Z^{5.8}$ scaling which is also reasonable. The corresponding harmonic contributions, however, proportional to $D^{[2]}$, are 10374.5 mHz and 312.9 mHz for $U_{7s,6p}$ and $W_{6s,5p}$, respectively, exploding any reasonable scaling relation. It should also be noted that for $U_{7s,6p}$ the harmonic and anharmonic contributions have the same sign, amplifying each other to give a total contribution of 13778.3 mHz to the PV vibrational shift, whereas the harmonic and anharmonic contributions to the $W_{6s,5p}$ shift oppose each other. It is hard to see how scaling laws can take into account such subtle effects, but on the positive side we note that the amplification of the PV vibrational shift when going from NWHFI to NUHFI is far beyond what could be expected from simple scaling laws.

Table 9 Individual orbital contributions (in mHz) to the PV vibrational shift of NUHFI

U	$2p_{1/2}$	$3p_{1/2}$	$4p_{1/2}$	$5p_{1/2}$	$6p_{1/2}$
$1s_{1/2}$	-4.3	22.7	-76.9	215.6	-880.5
$2s_{1/2}$	11.1	-58.8	199.5	-559.1	2282.6
$3s_{1/2}$	-19.1	100.9	-342.3	960.4	-3915.6
$4s_{1/2}$	29.8	-157.3	534.2	-1503.0	6100.5
$5s_{1/2}$	-47.3	249.8	-851.0	2420.6	-9685.6
$6s_{1/2}$	101.0	-533.1	1842.2	-5510.3	20871.5
$7s_{1/2}$	79.0	-414.9	1469.8	-4883.5	13778.3

Another electronic structure effect coming into play is that the uranium subvalence shell is more polarizable than the tungsten one. This can already be apprehended by looking at the electronic configuration of the metal atoms in the molecules. From projection analysis we find that tungsten has configuration $[Cd]5p^{5.97}5d^{3.95}6s^{0.44}6p^{0.49}$ and charge $Q^W = +1.2$ in NWHFI, whereas uranium has configuration $[Hg]5f^{2.66}6p^{5.81}6d^{1.80}7s^{0.31}$ and charge $Q^U = +1.3$ in NUHFI. The electronic configurations are given with respect to group 12 closed shell configurations in order to highlight a small, but significant difference in population of the $(n-1)p$ orbitals of the two metal atoms: Whereas in NWHFI the W $5p$ orbitals are complete, NUHFI displays a small U '$6p$ hole' due to overlap with ligand orbitals, as first observed in uranyl.[61]

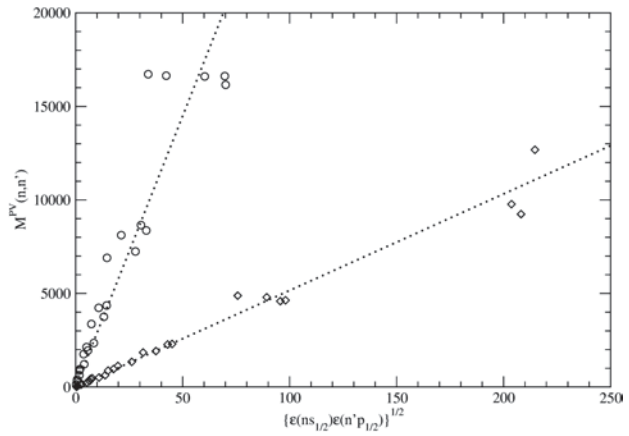

Fig. 2 Reduced PV matrix elements of uranium (circles) and tungsten (diamonds) as function of geometric mean of the orbital eigenvalues (see text for more details). All quantities are in atomic units. The straight lines have been obtained by a linear least square fit minimizing *relative* error.

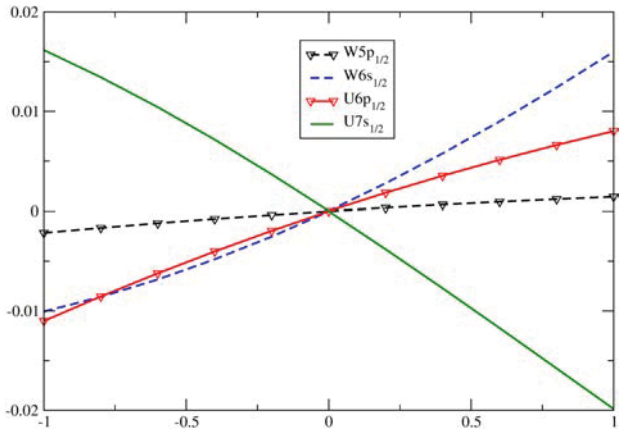

Fig. 3 Occupation of the W $5p_{1/2}/6s_{1/2}$ and the U $6p_{1/2}/7s_{1/2}$ orbitals, relative to the populations in the equilibrium structure, along the normal coordinate (in Å) associated with the $M \equiv N$ stretch.

More importantly, the occupation of the subvalence p orbital of uranium shows a stronger geometry dependence than that of its tungsten homologue. This is illustrated in Figure 3 where we show relative gross populations (from projection analysis) of the U $6p_{1/2}$ and $7s_{1/2}$ orbitals, as well as the homologous tungsten orbitals, along the the N≡M stretching mode of NMHFI. The variation of the U $6p_{1/2}$ population along the normal mode is less than for U $7s_{1/2}$, but on par with that of W $6s_{1/2}$, whereas the W $5p_{1/2}$ population is almost constant. This suggests that geometric derivatives of density matrix elements containing the subvalence p orbital will be larger for uranium than for tungsten. Indeed, when comparing Tables 8 and 9 we see more significant subvalence contributions to the shift for uranium than for tungsten.

5 Conclusions

A new class of chiral compounds of the form N≡UXYZ and N≡UHXY was investigated with the aim of assessing their suitability for experimental measurements of the PV effects using high resolution spectroscopy. Relativistic DFT calculations of the PV contribution to the vibrational transitions show that these are very promising candidates for future PV measurements, with PV effects in the Hz range for the fundamental N≡U stretching mode, more than an order of magnitude higher than for the earlier candidates. In addition, the stretching frequency of interest is conveniently located in the range of the CO_2 laser used for these high precision measurements. Although it might be difficult to isolate such compounds experimentally, as in the case of NUF_3,[21] they might still be trapped at ultra-cold temperatures to perform PV precision measurements, or more stable chiral uranium molecules could be designed and synthesized for further investigations.

In order to understand the nature of the large PV shifts in these systems, a detailed comparison of the homologous compounds NUHFI and NWHFI was performed. This analysis reveals that the difference in PV shifts by more than an order-of-magnitude in favor of the uranium compound can not be explained by a simple Z^5 scaling rule alone. Rather, the more extensive polarization of the uranium subvalence shell, as manifested by the $6p$ hole, and the strong geometry dependence of its occupation, due to overlap with ligands, seems to be the dominant factor. This finding puts an emphasis on the importance of consideration of the electronic structure effects in the design of candidate chiral molecules for the future PV detection experiments.

6 Acknowledgements

A.B. and A.-L.D. are thankful to D. Figgen for the valuable discussions and for the assistance. M.W. acknowledges funding by the Alexander von Humboldt foundation in terms of a Feodor-Lynen fellowship. T.S. acknowledges funding by the Agence National de Recherche (ANR; project NCPCHEM), including postdoc funding for M.O. The calculations for the analysis of parity violation shifts of NMHFI compounds were performed using HPC resources from CALMIP Hyperion cluster under CALMIP project P13154.

References

1 U. J. Meierhenrich, *Amino acids and the asymmetry of life*, Springer, Berlin, 2008.
2 J. Trost and K. Hornberger, *Phys. Rev. Lett.*, 2009, **103**, 023202.

3 B. Darquié, C. Stoeffler, S. Zrig, J. Crassous, P. Soulard, P. Asselin, T. R. Huet, L. Guy, R. Bast, T. Saue, P. Schwerdtfeger, A. Shelkovnikov, C. Daussy, A. Amy-Klein and C. Chardonnet, *Chirality*, 2010, **22**, 870–884.

4 F. De Montigny, R. Bast, A. S. P. Gomes, G. Pilet, N. Vanthuyne, C. Roussel, L. Guy, P. Schwerdtfeger, T. Saue and J. Crassous, *Phys. Chem. Chem. Phys.*, 2010, **12**, 8792–8803.

5 P. Schwerdtfeger, in *Computational Spectroscopy*, ed. J. Grunenberg, Wiley, 2010, ch. The Search for Parity Violation in Chiral Molecules, pp. 201–221.

6 M. Quack, J. Stohner and M. Wileke, *Annu. Rev. Phys. Chem.*, 2008, **59**, 741–769.

7 J. Crassous, C. Chardonnet, T. Saue and P. Schwerdtfeger, *Org. Biomol. Chem.*, 2005, **3**, 2218–2224.

8 C. Daussy, T. Marrel, A. Amy-Klein, C. T. Nguyen, C. J. Bordé and C. Chardonnet, *Phys. Rev. Lett.*, 1999, **83**, 1554–1557.

9 M. Ziskind, T. Marrel, C. Daussy and C. Chardonnet, *Eur. Phys. J. D*, 2002, **20**, 219–225.

10 J. Crassous, J.-P. Monier, F. Dutasta, M. Ziskind, C. Daussy, C. Grain and C. Chardonnet, *ChemPhysChem*, 2003, **4**, 541.

11 B. Y. Zel'dovich, D. B. Saakyan and I. I. Sobel'man, *JETP Lett.*, 1977, **25**, 94–97.

12 R. A. Harris and L. Stodolsky, *Phys. Lett. B*, 1978, **78**, 313–317.

13 D. W. Rein, R. A. Hegstrom and P. G. H. Sandars, *Phys. Lett. A*, 1979, **71**, 499–502.

14 J. K. Laerdahl and P. Schwerdtfeger, *Phys. Rev. A*, 1999, **60**, 4439–4453.

15 R. Bast, A. Koers, A. S. P. Gomes, M. Ilias, L. Visscher, P. Schwerdtfeger and T. Saue, *Phys. Chem. Chem. Phys.*, 2011, **13**, 864–876.

16 C. Stoeffler, B. Darquié, A. Shelkovnikov, C. Daussy, A. Amy-Klein, C. Chardonnet, L. Guy, J. Crassous, T. R. Huet, P. Soulard and P. Asselin, *Phys. Chem. Chem. Phys.*, 2011, **13**, 854–863.

17 D. Figgen, A. Koers and P. Schwerdtfeger, *Angew. Chem. Int. Ed.*, 2010, **49**, 2941–2943.

18 D. Figgen, T. Saue and P. Schwerdtfeger, *J. Chem. Phys.*, 2010, **132**, 234310.

19 P. Schwerdtfeger and R. Bast, *J. Am. Chem. Soc.*, 2004, **126**, 1652–1653.

20 N. Saleh, S. Zrig, T. Roisnel, L. Guy, R. Bast, T. Saue, B. Darquie and J. Crassous, *Phys. Chem. Chem. Phys.*, 2013, **15**, 10952–10959.

21 L. Andrews, X. Wang, R. Lindh, B. Roos and C. Marsden, *Angew. Chem. Int. Ed.*, 2008, **47**, 5366–5370.

22 M. Iliaš and T. Saue, *J. Chem. Phys.*, 2007, **126**, 064102.

23 L. Visscher and K. G. Dyall, *Atom. Data Nucl. Data Tabl.*, 1997, **67**, 207–224.

24 P. L. Anthony, R. G. Arnold, C. Arroyo, K. Bega, J. Biesiada, P. E. Bosted, G. Bower, J. Cahoon, R. Carr, G. D. Cates, J.-P. Chen, E. Chudakov, M. Cooke, P. Decowski, A. Deur, W. Emam, R. Erickson, T. Fieguth, C. Field, J. Gao, M. Gary, K. Gustafsson, R. S. Hicks, R. Holmes, E. W. Hughes, T. B. Humensky, G. M. Jones, L. J. Kaufman, L. Keller, Y. G. Kolomensky, K. S. Kumar, P. LaViolette, D. Lhuillier, R. M. Lombard-Nelsen, Z. Marshall, P. Mastromarino, R. D. McKeown, R. Michaels, J. Niedziela, M. Olson, K. D. Paschke, G. A. Peterson, R. Pitthan, D. Relyea, S. E. Rock, O. Saxton, J. Singh, P. A. Souder, Z. M. Szalata, J. Turner, B. Tweedie, A. Vacheret, D. Walz, T. Weber, J. Weisend, M. Woods and I. Younus, *Phys. Rev. Lett.*, 2005, **95**, 081601.

25 B. Noumeroff, *Publs. Obs. Central Astrophys. Russ.*, 1923, **2**, 188–288.

26 B. Noumerov, *Monthly Notices of the Royal Astronomical Society*, 1924, **82**, 592–601.

27 J. W. Cooley, *Math. Comput.*, 1961, **15**, 363–374.

28 A. D. Buckingham, *J. Chem. Phys.*, 1962, **36**, 3096–3096.

29 P. Schwerdtfeger, T. Saue, J. N. P. van Stralen and L. Visscher, *Phys. Rev. A*, 2005, **71**, 012103.

30 P. Schwerdtfeger, J. K. Laerdahl and C. Chardonnet, *Phys. Rev. A*, 2002, **65**, 042508.

31 D. Figgen and P. Schwerdtfeger, *Phys. Rev. A*, 2008, **78**, 012511.

32 V. Letokhov, *Physics Letters A*, 1975, **53**, 275–276.

33 A. D. Becke, *J. Chem. Phys.*, 1993, **98**, 5648–5652.

34 P. J. Stephens, F. J. Devlin, C. F. Chabalowski and M. J. Frisch, *J. Phys. Chem.*, 1994, **98**, 11623–11627.

35 M. J. Frisch, G. W. Trucks, H. B. Schlegel, G. E. Scuseria, M. A. Robb, J. R. Cheeseman, G. Scalmani, V. Barone, B. Mennucci, G. A. Petersson, H. Nakatsuji, M. Caricato, X. Li, H. P. Hratchian, A. F. Izmaylov, J. Bloino, G. Zheng, J. L. Sonnenberg, M. Hada, M. Ehara, K. Toyota, R. Fukuda, J. Hasegawa, M. Ishida, T. Nakajima, Y. Honda, O. Kitao, H. Nakai, T. Vreven, J. A. Montgomery, Jr., J. E. Peralta, F. Ogliaro, M. Bearpark, J. J. Heyd, E. Brothers, K. N. Kudin, V. N. Staroverov, R. Kobayashi, J. Normand, K. Raghavachari, A. Rendell, J. C. Burant, S. S. Iyengar, J. Tomasi, M. Cossi, N. Rega, J. M. Millam, M. Klene, J. E. Knox, J. B. Cross, V. Bakken, C. Adamo, J. Jaramillo, R. Gomperts, R. E. Stratmann, O. Yazyev, A. J. Austin, R. Cammi, C. Pomelli, J. W. Ochterski, R. L. Martin, K. Morokuma, V. G. Zakrzewski, G. A. Voth, P. Salvador, J. J. Dannenberg, S. Dapprich, A. D. Daniels, . Farkas, J. B. Foresman, J. V. Ortiz, J. Cioslowski and D. J. Fox, *Gaussian 09 Revision A.1*, Gaussian Inc. Wallingford CT 2009.

36 R. A. Kendall, T. H. Dunning and R. J. Harrison, *J. Chem. Phys.*, 1992, **96**, 6796–6806.

37 D. E. Woon and T. H. Dunning, *J. Chem. Phys.*, 1993, **98**, 1358–1371.

38 K. A. Peterson, D. Figgen, E. Goll, H. Stoll and M. Dolg, *J. Chem. Phys.*, 2003, **119**, 11113–11123.

39 M. Dolg and X. Cao, *J. Phys. Chem. A*, 2009, **113**, 12573–12581.

40 A. A. Clabo, Jr., W. D. Allen, R. B. Remington, Y. Yamaguchi and H. F. Schaefer III, *Chem. Phys.*, 1988, **123**, 187–239.

41 V. Barone, *J. Chem. Phys.*, 2004, **120**, 3059–3065.

42 DIRAC, a relativistic ab initio electronic structure program, Release DIRAC10 (2010), written by T. Saue, L. Visscher and H. J. Aa. Jensen, with contributions from R. Bast, K. G. Dyall, U. Ekström, E. Eliav, T. Enevoldsen, T. Fleig, A. S. P. Gomes, J. Henriksson, M. Iliaš, Ch. R. Jacob, S. Knecht, H. S. Nataraj, P. Norman, J. Olsen, M. Pernpointner, K. Ruud, B. Schimmelpfennig, J. Sikkema, A. Thorvaldsen, J. Thyssen, S. Villaume, and S. Yamamoto (see http://dirac.chem.vu.nl).

43 B. Schimmelpfennig, *AMFI, An Atomic Mean-field Spin-Orbit Integral Program, Stockholm, Sweden*, 1996.

44 T. Yanai, D. P. Tew and N. C. Handy, *Chem. Phys. Lett.*, 2004, **393**, 51–57.

45 C. Thierfelder, G. Rauhut and P. Schwerdtfeger, *Phys. Rev. A*, 2010, **81**, 032513.

46 K. Faegri, *Theor. Chim. Acta*, 2001, **105**, 252–258.

47 T. H. Dunning, *J. Chem. Phys.*, 1989, **90**, 1007–1023.

48 K. G. Dyall, *Theo. Chem. Acc.*, 2002, **108**, 335–340.

49 K. Dyall, *Theo. Chem. Acc.*, 2011, **129**, 603–613.

50 K. Dyall, *Theo. Chem. Acc.*, 2007, **117**, 491–500.

51 R. Holzwarth, T. Udem, T. W. Hänsch, J. C. Knight, W. J. Wadsworth and P. S. J. Russell, *Phys. Rev. Lett.*, 2000, **85**, 2264–2267.

52 M. B. Smith and J. March, *March's Advanced Organic Chemistry: Reactions, Mechanisms, and Structure*, Wiley-Interscience, Hoboken, NJ, 5th edn, 2001.

53 J. N. van Stralen, L. Visscher, C. V. Larsen and H. J. A. Jensen, *Chem. Phys.*, 2005, **311**, 81 – 95.

54 G. Knizia, *J. Chem. Theory Comp.*, 2013, **9**, 4834–4843.

55 M. A. Bouchiat and C. Bouchiat, *J. Physique*, 1974, **35**, 899–927.

56 I. B. Khriplovich, *Parity nonconservation in atomic phenomena*, Gordon and Breach Science Publishers, Philadelphia, 1991.

57 M. A. Bouchiat and C. C. Bouchiat, *Phys. Lett. B*, 1974, **48**, 111–114.

58 V. A. Alekseev, B. Y. Zel'dovich and I. I. Sobel'man, *Sov. Phys. Usp.*, 1976, **19**, 207.

59 A. N. Moskalev, R. M. Ryndin and I. B. Khriplovich, *Sov. Phys. Usp.*,

1976, **19**, 220.
60 M. Seaton, *Rep. Prog. Phys.*, 1983, **46**, 167–257.
61 P. Pyykkö and L. Laaksonen, *J. Phys. Chem.*, 1984, **88**, 4892–4895.